



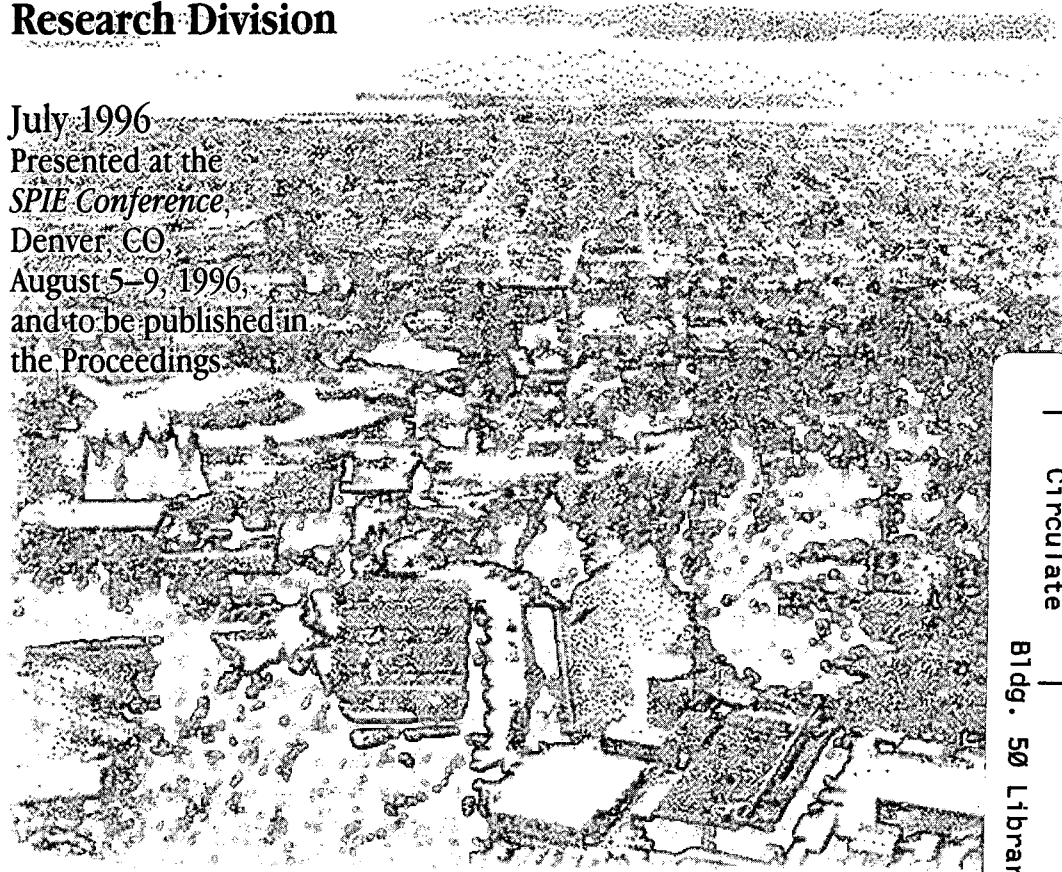
ERNEST ORLANDO LAWRENCE BERKELEY NATIONAL LABORATORY

Preliminary Optical Design of a Varied Line-Space Spectrograph for the Multi-Channel Detection of Near-Edge X-ray Absorption Fine Structure (NEXAFS) Spectra in the 280–550 eV Energy Range

B.S. Wheeler, W.R. McKinney, Z. Hussain,
and H. Padmore

**Accelerator and Fusion
Research Division**

July 1996
Presented at the
SPIE Conference,
Denver, CO,
August 5–9, 1996,
and to be published in
the Proceedings



REFERENCE COPY |
Does Not |
Circulate |
Bldg. 50 Library.

DISCLAIMER

This document was prepared as an account of work sponsored by the United States Government. While this document is believed to contain correct information, neither the United States Government nor any agency thereof, nor the Regents of the University of California, nor any of their employees, makes any warranty, express or implied, or assumes any legal responsibility for the accuracy, completeness, or usefulness of any information, apparatus, product, or process disclosed, or represents that its use would not infringe privately owned rights. Reference herein to any specific commercial product, process, or service by its trade name, trademark, manufacturer, or otherwise, does not necessarily constitute or imply its endorsement, recommendation, or favoring by the United States Government or any agency thereof, or the Regents of the University of California. The views and opinions of authors expressed herein do not necessarily state or reflect those of the United States Government or any agency thereof or the Regents of the University of California.

**PRELIMINARY OPTICAL DESIGN
OF A VARIED LINE-SPACE SPECTROGRAPH
FOR THE MULTI-CHANNEL DETECTION OF
NEAR-EDGE X-RAY ABSORPTION FINE STRUCTURE (NEXAFS)
SPECTRA IN THE 280-550 eV ENERGY RANGE***

Benjamin S. Wheeler, Wayne R. McKinney, Zahid Hussain, and Howard Padmore
Advanced Light Source, Lawrence Berkeley National Laboratory
University of California, Berkeley, California 94720

Light Source Note:	
Author(s) Initials	RW 7/24/86 Date
Group Leader's initials	AMP 7/30/86 Date

Preliminary optical design of a varied line-space spectrograph for the multi-channel detection of Near-Edge X-ray Absorption Fine Structure (NEXAFS) spectra in the 280 - 550 eV energy range

Benjamin S. Wheeler, Wayne R. McKinney, Zahid Hussain, and Howard Padmore

Lawrence Berkeley National Laboratory, Berkeley California

ABSTRACT

The optical design of a varied line-space spectrograph for the multi-channel recording of NEXAFS spectra in a single "snapshot" is proposed. The spectrograph is to be used with a bending magnet source on beamline 7.3.2 at the Advanced Light Source (ALS). Approximately 20 volts of spectra are simultaneously imaged across a small square of material sample at each respective K absorption edge of carbon, nitrogen, and oxygen. Photoelectrons emitted from the material sample will be collected by an electron imaging microscope, the view field of which determines the sampling size. The sample also forms the exit slit of the optical system. This dispersive method of NEXAFS data acquisition is three to four orders of magnitude faster than the conventional method of taking data point-to-point using scanning of the grating. The proposed design is presented along with the design method and supporting SHADOW raytrace analysis.

Keywords: NEXAFS, synchrotron optics, varied line-space gratings

1. INTRODUCTION

Every optical system can be described in terms of some set of parameters that define it--the distances between elements, their orientations, and shapes. The problem of geometrical optical design is to find a set of parameter values that will produce a desired image. Ideally the optical system can be modeled analytically, so that the optical behavior of the system can be expressed in equations that provide insight into the role of each parameter in the imaging of the system. A set of parameter values can then be chosen based on these equations. Unfortunately, most complicated systems cannot easily be analytically solved--there are no equations and therefore no insight. In these cases it is necessary to turn to the raytrace; complex, numerical, and exact, but a black box as far as the designer is concerned. The design problem becomes one of tedious and time-consuming trial-and-error, best performed by computer.

This paper will outline a design method for a three-element optical system consisting of two spherical mirrors and a plane varied line-space (VLS) grating, which is to be used for NEXAFS spectroscopy. The design problem poses a number of challenges. First, it is difficult to construct a simple analytical model that adequately models the optical system. This forces the use of a complex raytrace to model the optical behavior of the system. Second, the system is described by a large number of parameters, most of which affect the behavior of the system, and many of which are themselves related through other quantities significant to the design. The raytrace allows only trial-and-error analysis, a time consuming task even when done by computer. Finally, the specifications call for many characteristics that are themselves somewhat mutually exclusive: large aperture size and small spot size, low dispersion and high resolving power. These contradictions force continual trade-off and compromise.

Varied line-space grating systems historically arose from the development of exacting control systems for ruling engines^{1, 2}. An engine with electronic feedback control to guarantee exact placement of equally spaced grooves already has most of the necessary capabilities for ruling VLS gratings. VLS gratings have seen application in astrophysical applications for many years³. A very fruitful relationship has existed between the space program in the United States and two companies, Hitachi in Japan and Perkin Elmer in California. The principals have been T. Harada and T. Kita in Japan and G. Hirst in the United States. The main proponent and designer of VLS systems over the last decade, M. Hettrick, provided feedback so that excellent VLS gratings could be manufactured.

VLS systems, which have been slow to be accepted by the synchrotron light source community in general, have been championed in the United States by the Center for X-ray Optics (CXRO)(Hettrick, Underwood, and Koike)⁴ at Lawrence Berkeley National Laboratory (LBNL), and in Japan by Hitachi (Harada and Kita)⁵⁻⁷. VLS systems are in place on the experimental floor of the ALS^{8, 9}. They achieve excellent resolving power, and also achieve significant cost savings since they stay in focus over a very wide energy range, and do not require moving slits to maintain focus. To our knowledge, a VLS system is operational at the Synchrotron Radiation Center in Madison Wisconsin^{10, 11}, and another at the Center for

Advanced Microstructures and Devices (CAMD) in Louisiana¹². The gratings for these instruments were ruled by Hyperfine in Boulder, Colorado. The Richardson Grating Laboratory in Rochester New York (formerly Milton Roy Co.) also has the capability to rule VLS gratings, and has made them for internal evaluation.

There have been concerns that ruled VLS gratings might not give the required stray light performance at soft X-ray wavelengths when used with a bright continuous source like a synchrotron bending magnet. Ruled VLS gratings share the same increasing stray light from random groove misplacement as ruled non-VLS gratings. Recently several vendors have pursued the construction of VLS gratings by holographic methods, which may address this concern. Tayside Optical in the UK, Shimadzu in Japan, and Zeiss in Germany have interest in this method. If holographic VLS gratings can be produced with good "blaze" efficiency, it will help speed the acceptance of VLS systems.

This paper develops the design work in a manner to promote understanding for those facing a similar problem. Section 2 provides an overview of the optical system, its geometry, and the parameters that define it. Section 3 briefly outlines the optimization algorithm used in the work, the simplex method. In Section 4 the merit function is developed, including the optical model and some important calculations. Section 5 discusses the choice of optimization variables, and Section 6 explores the problems and compromises required in choosing a design. Section 7 presents a design and reviews its performance, and Section 8 concludes the paper.

2. THE OPTICAL SYSTEM

NEXAFS spectroscopy is an atom-specific technique that probes the electronic structure of the selected atom near the valence level. Atomic specificity is achieved through selection of an absorption edge (e.g., K or L shell) of an atom of interest. The technique is particularly useful in probing bonds to intra-molecular and, to lesser degree, extra-molecular neighbors (e.g., surface atoms). The method has special capabilities to detect the presence of a specific bond in a molecule and map the orientation of the molecule or functional group adsorbed on the surface or present in solids¹³. It can also tell which orbitals are involved in bonding to the surface.

The conventional method for NEXAFS measurement uses synchrotron radiation from a tunable monochromator which falls on a sample after passing through a grid. The total or partial electron yield signals from the sample as well as from the grid are measured as the monochromator is scanned in small photon energy intervals through an atomic absorption edge of interest to obtain a NEXAFS spectrum over an energy width of about 15-30 eV. However, there are many advantages (specifically related to time-resolved spectroscopy) if it is possible to obtain a complete NEXAFS scan in one "snapshot". This paper describes a straightforward existing technology to achieve this goal.

The idea is an extension of the method which has been used for decades in optical spectrographs. Gerritsen¹⁴ has demonstrated in principle the technique of obtaining a complete NEXAFS scan in one shot using a laser-produced plasma source in the soft x-ray energy range. One exposes the sample with a well-defined, dispersed spectrum of radiation and uses an imaging electron microscope to detect the total yield electron signal, which will in turn spatially resolve the position from which the electrons are emitted. Each location (more precisely line) on the sample corresponds to excitation from a different photon energy. The resolution achieved by Gerritsen et al. using a laser plasma source was about 7 eV. The goal of this work is to develop a bending magnet branchline spectrograph, which when used in conjunction with an electrostatic electron microscope having a magnification of ≈ 20 , a resolution of ≈ 5 micron, and a field of view of $0.5 \text{ mm} \times 0.5 \text{ mm}$ will allow the implementation of this technique¹⁵. The spectrograph should maintain a resolving power of greater than 1500 in the recording of a 15-20 eV wide "single shot" NEXAFS spectrum with $\approx 1\%$ statistics in about a millisecond in the soft x-ray energy range (280-550 eV). Although this technique presumes a homogeneous sample over roughly 0.25 mm^2 , it is possible to treat inhomogeneous materials by rotating or oscillating the sample at an appropriate rate and time-averaging the signal. Finally, the spectrograph will be designed to provide these "snapshots" at each of the three K absorption edges of carbon, nitrogen, and oxygen by suitable rotation of the grating.

The spectrograph will consist of a Kirkpatrick-Baez¹⁶ (K-B) mirror system in series with a plane VLS grating. The Kirkpatrick-Baez mirror configuration consists of two spherical or cylindrical mirrors whose normals are perpendicular, shown in Figure 1.

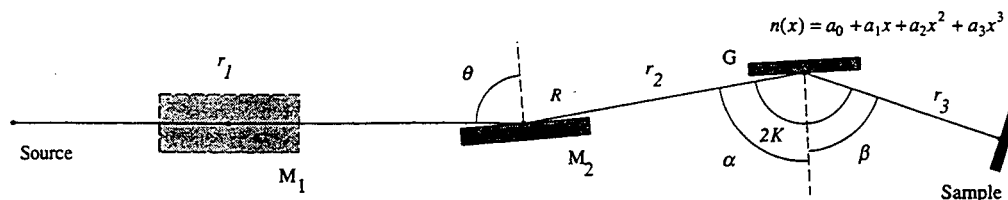


Fig. 1. The three element system geometry and variables (side view)

Distances between elements are measured along the pole ray. The distance from the source to the vertically focusing mirror (M_2) is denoted r_1 . The M_2 -grating separation is then r_2 , and the grating-sample distance is r_3 . θ and R denote the mirror incidence angle and radius, respectively. The grating groove pattern is described by the polynomial

$$n(x) = a_0 + a_1x + a_2x^2 + a_3x^3, \quad (1)$$

where n is groove frequency in grooves per millimeter, and x is the coordinate on the grating as measured from the element pole in the dispersion plane. a_0 denotes the fundamental groove frequency, with a_1 , a_2 , and a_3 labeling the VLS coefficients. α and β denote the incident and reflected angles, respectively, again as measured from the element normal. We follow the signed angle convention of Palmer and McKinney¹⁷ where angles on the source side of the normal are negative. The grating coordinate is therefore taken as negative for points on the near side of the grating relative to the source and positive for points on the far side. The diffracted order of the grating is m , with inner orders corresponding to positive values of m , and vice versa. K is chosen to denote the half deviation angle.

The K-B grating configuration has a number of features that make it attractive for design and use. The first, and most important for this work is the almost complete separation of the vertical and horizontal focusing of the mirrors. This characteristic is crucial because it allows the horizontal and vertical design to be considered separately—instead of one three-element design problem in three dimensions, there is one one-element problem in one dimension (the horizontal mirror) and one two-element problem in one dimension (the vertically focusing mirror and grating). This not only allows the use of standard wavefront aberration theory in the design of the horizontal mirror, but more importantly it permits the use of only a two-dimensional raytrace in the design of the two-element system, a simplification vital to the computer implementation of the numerical design method. The rest of this paper will largely be concerned with the two-element design, as one-element design methods are well established.

The other advantage of the Kirkpatrick-Baez system, held in this case over spherical grating systems, is that in the dispersion plane the focusing and dispersion are separated. This is useful if the grating is to rotate to scan different energies across a exit slit, or in this case to focus different energy ranges on a sample. In a spherical grating monochromator, dispersion and focusing are not separated, so that when the grating is rotated, the focal plane rotates with it, altering the focal characteristics at the (stationary) exit slit¹⁸. This effect is eliminated in the K-B configuration.

3. THE SIMPLEX ALGORITHM

Since the two-element system cannot easily be described analytically, it must be modeled numerically. The numerical optical model leaves the designer with a black box into which parameter values are entered, and out of which comes an image profile. The simplest way to use this for design would be to select random sets of parameters and run the model, examining the results until a satisfactory one is found—simple, but tremendously inefficient. A more efficient method would be to choose a initial set of parameter values and then adjust them, comparing the results of each adjustment with preceding systems until a satisfactory one is found. This form of iterative trial-and-error is still simple, yet much more efficient than blind guessing. Better still, it is a problem ideally suited to solution by computer, and several algorithms already exist. The Simplex Method of Nelder and Mead (reviewed by Caceci¹⁹ and explained further by Palmer²⁰) is perhaps the simplest, yet very effective.

The simplex algorithm, also known as the amoeba algorithm to distinguish it from the simplex of linear programming, was developed as a general solution to the problem of fitting curves to a set of numerical data. One often wishes to determine a set of unknown parameter values in an equation such that a set of independent and dependent variable values satisfy a known relation. Most often an equation is known from theory (the known relation), and a set of numerical data from mea-

surement forms the set of independent and dependent variables. The task is to find the set of parameters values such that the measured data lies on the theoretical function curve¹⁹.

This is most commonly achieved by choosing a response surface, to be minimized, according to the following scheme. The parameters to be fit define a parameter space: M parameters define a space of M dimensions. An additional dimension is added to this space, which spans a function of the parameters, yielding a space of dimension $M+1$. This function, called the merit function, describes a surface whose value depends on position in parameter space. The merit function/surface is generally chosen so that lower values correspond to better fit: this assignment is arbitrary, but easier to deal with than the opposite arrangement--perfect fit then gives a merit value of zero as opposed to infinity^{19, 20}.

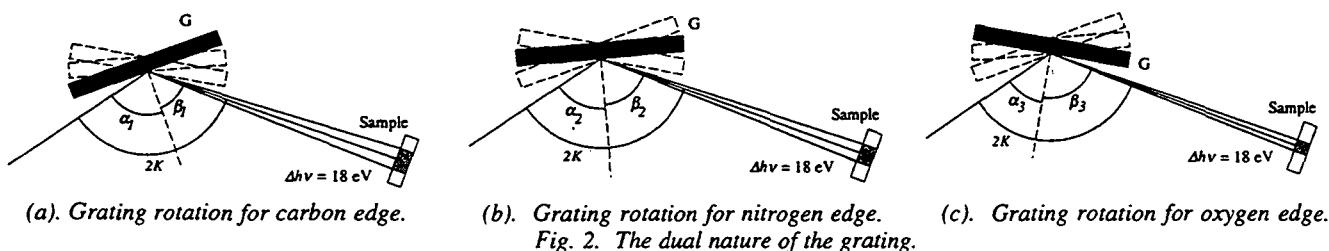
The simplex itself is a polyhedron defined in the M -dimensional parameter space, comprised of a set of vertices with one more vertex than the number of dimensions spanning the space ($M+1$). The simplex is constructed by choosing a single point in parameter space (corresponding to a set of parameter values) as an initial vertex, and then building a polyhedron containing $M+1$ vertices by adding vertices at a multiple of each of the set of unit vectors that spans the parameter space. Once the simplex is constructed, it calculates the response value corresponding to each of its vertices and moves in parameter space according to a carefully designed set of rules until it finds a set of parameter values that provide a minimum of the response surface. This procedure is exactly the same for optical design. Some measure of optical quality is used as the response surface, and the simplex is used to explore parameter space until a minimum is found.

The simplex is well suited to our problem for a number of reasons. First, it is conceptually simple, and therefore fairly easy to code and test. Second, it uses only evaluations of the merit function, not its derivatives. The merit function needs only be single valued for all points of parameter space, not continuous or differentiable. Finally, the algorithm is easily controlled to prevent divergence.

4. THE MERIT FUNCTION

From the point of view of the designer, the simplex algorithm merely automates the trial-and-error process through evaluations of some generalized merit function. All of the optics, all of the modeling and all of calculations are hidden in the merit function, which returns a single number for use by the simplex. The choice of the merit function is therefore crucial to the final result. The simplex is relentless in finding local minima in the merit function, but this relentlessness is a two-edged sword: the simplex will find minima no matter how wrong the model is, and it will produce good quality systems no matter how mistaken a version of optics it is given. However, apply a raytrace like SHADOW²¹ or build that system, and a fundamental fact quickly surfaces: if the model represented by the merit function differs from reality in any way, then the real image will reflect that difference. This gap between result and reality makes choosing a satisfactory design even more difficult, and must be guarded against with repeated use of independent testing, preferably with a quality commercial-grade raytracing program. Unfortunately the need for an accurate model of the optical system must be balanced with the computational burden that more accurate models impose, particularly given the nature of the simplex algorithm. An optimization may require several hundred iterations of the simplex, each requiring ten or more calls of the merit function, a load which adds up quickly, even with a powerful PC or workstation.

In order to understand how the model works, it is helpful to first explain how the optical system functions on an general, intuitive level. The NEXAFS experiment requires that roughly 20 eV be spread over a small material sample at the image plane. In this sense the system functions as a spectrograph--the grating is stationary, dispersing diffracted light over a length in the image plane. If a single K edge were to be treated, no further discussion would be necessary, however it is obviously much more efficient to design the optics to be capable of recording more than one absorption edge. To do this one merely rotates the grating until the desired energy range is focused onto the material sample. In this sense, the system functions as a constant deviation angle (CDA) monochromator, whose exit slit is defined by the finite field of view of the electron imaging microscope. This action is shown in Figs. 2 (a), (b), and (c).



To accurately model this system and insure a design which is truly optimized, this dual nature of the system must be considered. The model must rotate the grating appropriately for each K edge, then perform the raytrace across the source at each of a range of wavelengths before moving on to the next edge. This insures that the system will be optimized for all of the wavelengths involved and that the optimization will include by definition the effects that result from the rotation of the grating. Since this behavior is all hidden in the merit function, and since so many of the calculations necessary for design are also embedded here, it is convenient to review the structure of the merit function. The calculations in the merit function are divided roughly into three parts: first, those calculations depending on neither wavelength nor the rotation of the grating. Second, calculations that change with each rotation of the grating, but do not change over the range of wavelengths within each repositioning of the grating, and finally, those calculations that depend on wavelength.

The radius of the vertically focusing mirror does not depend on wavelength, so it is calculated first. For this the mirror can be treated as a single element, and wavefront aberration theory can then be used to calculate the radius such that the defocus will be zero at the sample. This is accomplished using the defocus aberration coefficient²² $F_{20} = 0$, where for a mirror,

$$F_{20} = \frac{1}{2} \left(\frac{\cos^2 \theta}{r_1} + \frac{\cos^2 \theta}{r_2 + r_3} \right) - \frac{\cos \theta}{R}. \quad (2)$$

The rotation of the grating is modeled by calculating the incident and diffracted angles for the grating, α and β , at the central wavelength of each absorption edge. For this the constant deviation geometry is used, where

$$\alpha = \sin^{-1} \left(\frac{a_0 m \lambda}{2 \cos K} \right) + K, \quad (3)$$

and

$$\beta = \sin^{-1} \left(\frac{a_0 m \lambda}{2 \cos K} \right) - K. \quad (4)$$

This calculation determines the position of the grating, which also fixes the source-size limit and the reciprocal linear dispersion for the system. The reciprocal linear dispersion is defined as the change in wavelength seen in the image plane for an infinitesimal change in position in the image plane along the dispersion direction. This quantity serves both as a measure of how much the grating disperses light of different wavelengths, as well as a conversion factor for converting distances in the image plane to wavelength units¹⁸. It is given by the equation,

$$\delta_r = \frac{\cos \beta}{a_0 m r_3}. \quad (5)$$

The source-size limit is defined as the image size in the focal plane of the source. It is a fundamental focusing limit which results from the magnification of the finite source by the system, and is defined by the equation,

$$\Lambda_s = M_g M_m \sigma_x, \quad (6)$$

where σ_x is the r.m.s. source size in the vertical direction, M_m is the mirror magnification, and M_g is the magnification of the grating in the dispersion direction.

For each position of the grating, the model samples a number of wavelengths across a range on either side of the central edge wavelength. At each of these wavelength samples, the source is modeled and then traced through the system. In order to ensure adequate correspondence between the optimizer and real systems, we model the synchrotron source as accurately as possible—experimentation with the model has shown this to be worthwhile even at a heavy price in computer run-time. This is accomplished by creating a sample of rays at each wavelength that is Gaussian in both dimension and angle. For both angle and spatial dimensions, the parameter values of the Gaussian function are calculated from the characteristics of an ALS bending magnet port. Each of the rays is then traced through the two-dimensional raytrace and its image coordinate calculated. The standard deviation of the ray coordinates is calculated, then converted from distance to wavelength units by multiplying by the linear reciprocal dispersion as calculated for the wavelength's central edge wavelength (Eq. 5).

The result is a list of r.m.s. image coordinate values, each corresponding to a wavelength sample across three edges, converted to spectral units. This list is sorted, and the worst one is returned as the merit value. This choice of optical merit becomes clear with a quick look at the equation defining resolving power, given by,

$$R \equiv \frac{\lambda}{\Delta\lambda} = \frac{\lambda}{\delta_r w_{rms}}, \quad (7)$$

where δ_r is the reciprocal dispersion and w_{rms} is the full-width r.m.s. image size. The resolving power is the true measure of a dispersive system's optical quality, however it is a quantity for which larger values correspond to higher quality systems. The simplex as it is defined here finds minima, so to maximize the resolving power, the simplex is used to find the minimum of the denominator--the full width r.m.s. spot size, converted to wavelength units. We denote this

$$merit = \delta_r w_{rms} \Big|_{worst}. \quad (8)$$

The choice of the largest spot size across all of the wavelengths insures that the simplex will optimize the system "from the bottom up"--always changing the parameters so that the worst spot size gets better. Averages or other statistical quantities are not as well suited, primarily because they ignore the absolute nature of the resolving power requirement: an average can be quite good even though several of its components are not.

5. VARIABLES OF OPTIMIZATION

The simplex algorithm allows complete freedom in choosing which system variables should be optimized, and this selection deserves some discussion. Like the merit function, the optimization variables must be chosen carefully to insure the simplex does not misunderstand the nature of the problem. If the simplex is given variables that are in any way related, secondary effects may arise in the merit function and lead to unpredictable behavior in the optimizer. Further, the simplex is a local optimizer--the smaller the number and scope of parameter values it is given, the more effective it is likely to be. The choice of optimization variables should therefore correspond as exactly as possible to the optical problem that the simplex is being called upon to solve.

With this in mind, the system parameters are divided roughly into three separate categories: user selected parameters, selected "arbitrarily" by the designer; calculated parameters, calculated from user selected parameters; and optimizer parameters, those parameters which will be used by the simplex. For this system, the designer-selected parameters are chosen to be r_1 , r_2 , r_3 , θ , K , a_0 , and the diffracted order m . From these the calculated parameters can be found, consisting of α , β , and R . Finally, the grating groove pattern coefficients a_1 , a_2 , and a_3 are chosen as the variables of optimization.

This division of parameters is based primarily on the premise that for each arrangement of the system (i.e. for each set of r_1 , r_2 , r_3 , θ , K , and a_0) there exists a set of grating groove pattern coefficients that best corrects the aberrations of that system²². Since each arrangement will result in different aberrations and therefore a different set of grating coefficients to correct those aberrations, this division is quite natural. r_3 , K , and a_0 are fixed for another reason as well: each of these affects the reciprocal dispersion, which is an important design specification, so these parameters must remain in the designer's direct control. Finally, the calculated parameters: again α and β fall naturally into this category based on the nature of the optical system. The decision to focus the mirror at the sample is based on the need to reduce the mirror aberrations as much as possible. Other designers have manipulated the mirror radius to decrease the magnification of the source even further²³, but unfortunately this technique is not possible in this case, as the requirement for a large aperture will not allow sufficient correction of the resulting increase in mirror aberrations.

For all its intuitive basis, this division of variables does carry some complication. Although it is true that for each arrangement there probably exists a set of grating coefficients that will best correct the mirror aberrations of that arrangement, it is also true that different placements will themselves affect the spot size and resolving power. The optimizer has simplified the design problem to the choice of placement and orientation of the elements, but which such placement is best? Although again the optical model is of no help except for trial and error, this choice can be made using some experimentation with the optimizer, and some intuition about the dispersion and the source-size limit.

6. CHOOSING A DESIGN

The secondary optimization that lies in the selection of a system layout is more complicated than that of the grating, largely because of the effects that result from relations between the parameters involved. Since resolving power is perhaps the most important measure of the quality of a dispersive optical system, it is a natural place to begin our analysis. Recall that the resolving power is defined by the equation,

$$R \equiv \frac{\lambda}{\Delta\lambda} = \frac{\lambda}{\delta_r w_{rms}} \quad (9)$$

The wavelengths are fixed by the experiment, leaving two factors which directly control the resolving power: the full-width r.m.s. spot size and the reciprocal dispersion of the grating.

The r.m.s. spot size results from the convolution of two separate quantities, the source-size limit and the optical aberrations of the system. The source-size limit can be analytically expressed, and although the aberrations cannot, experience with the optimizer can be used to draw some general conclusions so that both may be analyzed. Combining this analysis with the specifications from the NEXAFS experiment, it is possible to eliminate large areas of parameter space, an effort well worth the reduction in computer run-time.

The source-size limit results from the finite dimension of the synchrotron source, magnified by the system, and is composed of three separate parts: the actual size of the source, the magnification of the mirror, and the magnification of the grating (Eq. 6). The source itself is fixed, leaving the element magnifications as the only variables. Clearly a small source-size limit requires that the system demagnify: the source-size limit will be small when the combined total magnification $M_m M_g$ is small.

Despite the lack of a satisfactory two-element theory, repeated runs and experimentation with the optimizer allow us to make three generalizations about the aberrations of the system. First, the aberrations appear to reach a minimum when the mirror magnification approaches unity. Second, aberrations terms are strongly coupled to the aperture size of the system. Third, aberrations increase with incidence angle, as measured from the element normal. The first conclusion is of primary concern, because it reveals a fundamental conflict between the source-size limit and the optical aberrations. Strong mirror demagnification provides a small source-size limit but large aberrations, and near unity mirror magnification provides smaller aberrations but a large source size limit. This conflict is further complicated by the magnification due to the grating. Since the design will require determining which magnification will optimize this conflicting relationship between source-size limit and aberrations, it is helpful to explore the system magnification in more detail. This treatment is not meant to be exhaustive, but rather serves to introduce the issues in selecting a design.

The magnification M of the system is the result of the combined magnification of the separate elements, and is given by $M = M_m M_g$. The mirror magnification is given by,

$$M_m = \frac{r'_m}{r_m} = \frac{r_2 + r_3}{r_1} \quad (10)$$

and the grating magnification is defined as,

$$M_g = \frac{r'_g \cos \alpha}{r_g \cos \beta} \quad (11)$$

The magnification of the mirror depends only on the relative position of the image and object. Since we have stipulated that the mirror focus at the sample, the grating image and object distances are equal and their ratio unity, so only the ratio of cosines are left. The grating magnification therefore depends exclusively on the rotation of the grating, which is in turn influenced by wavelength, the diffracted order, and the groove frequency (Eqs. 3, 4). For positive (inner) diffracted order, large groove frequencies translate into a larger α and smaller β . Since both are near grazing, the ratio of their cosines becomes smaller, in turn bringing down the grating magnification and the total system magnification. The opposite happens for negative (outer) orders. In this case higher groove frequency translates into smaller α and larger β values, which increase the grating magnification and total system magnification. These changes in magnification will affect both the aberrations and the

source-size limit, and it is probable that there exists some set of user-selected parameters that correspond to a value of the magnification for which both the source size-limit and aberrations are minimized.

Unfortunately, matters are complicated further by the second component of the resolving power, the reciprocal dispersion. The reciprocal linear dispersion converts the spot size to wavelength units, and is given by Eq. 5. For high resolving power it is necessary that the reciprocal dispersion be small. The diffracted order will be either positive or negative one, and while it has no explicit effect on the reciprocal dispersion, it does implicitly through β . The grating-sample distance r_3 appears only explicitly in the denominator--large separations translate into higher resolving power. The groove frequency appears not only explicitly in the reciprocal dispersion, but implicitly in β as well: for positive diffracted orders, larger groove frequencies translate into smaller values of β , resulting in turn in an increase in $\cos\beta$ and the reciprocal dispersion. Conversely, for negative diffracted orders, larger groove frequencies translate to larger values of β , smaller $\cos\beta$ and larger resolving power. However, regardless of diffracted order, this relatively minor effect is offset by the explicit appearance of the groove frequency in the denominator--larger groove frequencies therefore translate into smaller reciprocal dispersion, and in turn higher resolving power.

The final layer of complication is added when the specifications for the system are considered: low dispersion, large aperture, high efficiency. Each of these presents a dilemma for the designer. Low dispersion is necessary to meet the demands of the detector, yet this comes directly at a price in resolving power. A large aperture will collect more light and provide for later use of off-axis polarizations, but at a cost in aberrations. Efficiency in x-ray optics means grazing incidence, again at a price in aberrations.

Despite the largely unknown relation between the system magnification and its aberrations, it should be possible to find a value of the magnification that represents an optimum balance between the source-size limit and the aberrations. Ideally we would use the following program to find this optimal value:

1. Determine the set of r_1, r_2, r_3, a_0, m values that result in a system magnification that best balances the source-size limit and the optical aberrations.
2. Determine the best $a_0, r_3,$ and m values that will maintain the balance of (1) and also find the optimal compromise between the low dispersion required and the high dispersion needed for high resolving power.
3. Determine the largest system aperture and largest incidence angles that will allow (1) and (2).

To explore all of the possible solutions of this problem represents the search of a prohibitively large area of parameter space, complicated by the many relations between parameters. To simplify the problem, we choose parameter values according to the following scheme:

- a. Reasonable values for the aperture, the incidence angles, and the source-mirror distance r_1 are chosen from consideration of the specifications.
- b. The groove frequency a_0 and grating-sample distance r_3 are chosen to provide a reasonable dispersion for the detector view field.
- c. The mirror-grating separation r_2 is optimized to find the mirror magnification which provides the best balance of source-size limit and aberrations.

The first set of parameters (*a*) are independent of both the magnification conflict and the dispersion conflict, so they are fixed to simplify the problem. The second set (*b*) represents the primary control of the dispersion of the system. Since this is both an important specification and optical quantity, a set of values is chosen based on the analysis above. This leaves the mirror-grating separation. Since this parameter is independent of most other specifications (notably dispersion) it provides an excellent way to control the magnification of the system. Trial-and-error in this case requires optimizing the grating with the simplex for each choice of r_2 , a tedious task that immediately suggests computer solution. The simplex is again a natural choice, simple to implement although it now represents a major computing burden. In optimizing the mirror-grating separation, each merit function call involves the simplex optimization of the grating coefficients outlined in Section V. However, although the optimizer may take many hours to run, it is still faster and simpler than manual methods. This combination of elimination and optimization reduces the amount of blind trial-and-error significantly, but it is still necessary to adjust both the aperture size and the groove frequency to fine-tune the dispersion and resolving power of the system.

7. THE DESIGN

For this optimizer run, five energies were sampled across a 30 eV range at each absorption edge. 441 rays (21 spatial x 21 angular) were sampled across the Gaussian source at each wavelength. The initial simplex vertices were chosen to be $\{r_2\} = \{3000\}$ and $\{a_1, a_2, a_3\} = \{0, 0, 0\}$ for the magnification and grating optimizations, respectively. The grating optimizer was set to terminate after 500 iterations and the magnification optimizer after 150, resulting in a run-time of some 14 hours. The program is implemented in C++ and was run on a Macintosh PPC 7200/75. The optimized design is given below.

Optical System Parameters:

r1 (mm):	14000.0000	theta (deg):	87.0000
r2 (mm):	4152.4414	a0 (g/mm):	900.0000
r3 (mm):	800.0000	a1 (g/mm ²):	2.2463e+00
R (mm):	139801.5713	a2 (g/mm ³):	4.5721e-03
m:	1	a3 (g/mm ⁴):	7.2351e-06
K (deg):	87.0000		

Wavelength Data:

Edge (eV):	Alpha (deg):	Beta (deg):		
p ₀ (mr):	Target (mm):	Accept (mr):		
<u>Energy (eV)</u>	<u>Spot (mm)</u>	<u>R. Power</u>	<u>S. Size (mm)</u>	<u>S.S. Limited R.P.</u>
276.0	0.005784	3145.42	0.002377	7654.76
283.5	0.005658	3130.37	0.002377	7452.25
291.0	0.005539	3114.95	0.002377	7260.18
298.5	0.005428	3099.20	0.002377	7077.77
306.0	0.005323	3083.15	0.002377	6904.29
Edge (eV):	Alpha (deg):	Beta (deg):		
p ₀ (mr):	Target (mm):	Accept (mr):		
<u>Energy (eV)</u>	<u>Spot (mm)</u>	<u>R. Power</u>	<u>S. Size (mm)</u>	<u>S.S. Limited R.P.</u>
392.0	0.004456	3255.85	0.004481	3237.89
399.5	0.004506	3159.52	0.004481	3177.11
407.0	0.004561	3064.19	0.004481	3118.56
414.5	0.004615	2973.45	0.004481	3062.13
422.0	0.004669	2887.03	0.004481	3007.71
Edge (eV):	Alpha (deg):	Beta (deg):		
p ₀ (mr):	Target (mm):	Accept (mr):		
<u>Energy (eV)</u>	<u>Spot (mm)</u>	<u>R. Power</u>	<u>S. Size (mm)</u>	<u>S.S. Limited R.P.</u>
522.0	0.006930	1710.06	0.006055	1957.20
529.5	0.006980	1673.81	0.006055	1929.48
537.0	0.007029	1638.88	0.006055	1902.53
544.5	0.007078	1605.20	0.006055	1876.33
552.0	0.007126	1572.71	0.006055	1850.83

The first section of the output represents the optimized set of system parameter values, and the second set summarizes the optical performance of the optimized system across all of the energy samples. The quantities displayed at each edge are as follows. *Edge* refers to the central edge energy used for each energy range. *Alpha* and *Beta* are the grating incidence and diffraction angles, respectively, at each edge energy. *p₀* denotes the r.m.s. angular width of the synchrotron source at each edge energy. *Target* refers to the linear distance in the image plane over which 18 eV is dispersed. *Accept* is the full-width angular acceptance of the system. At each energy within the edge the r.m.s. spot size (*Spot*), resolving power (*R. Power*), source-size limit (*S. Size*), and source-limited resolving power (*S. S. Limited R.P.*) are displayed. In both cases the spot size refers to the r.m.s. width, while the resolving power is calculated from twice the r.m.s. image width.

A few calculations remain. First, the horizontal mirror must be added to the design. The horizontally focusing mirror is placed 7000 mm from the source, inside the ALS shield wall. The mirror radius is calculated to correct the horizontal defocus at the sample, according to Eq. 2, yielding a radius of $R = 168701.651$ mm. Finally, the element lengths must be calculated to give the acceptance chosen in the design. For accuracy this is done using the SHADOW element footprints. The horizontally focusing mirror is 1000 mm long; the vertically focusing mirror is 137.6 mm long, and the grating is 74 mm long.

To verify the validity of the design, we use SHADOW to raytrace the complete three-dimensional system. In Fig. 3 (a - i) we show the spot diagrams in the image plane at 3 energies for each edge.

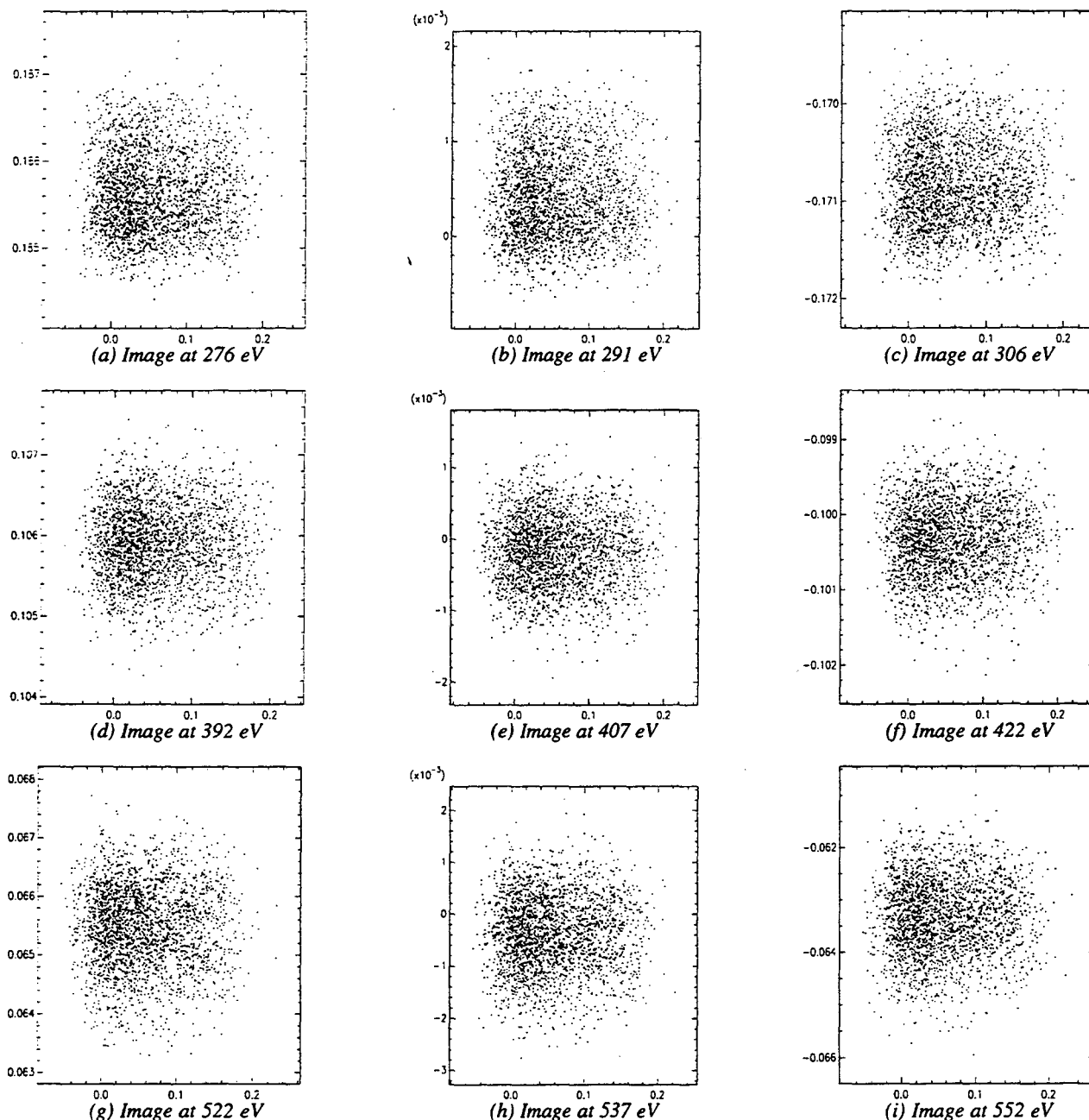


Fig. 3. SHADOW plots. 2500 rays each plot, units are centimeters.

The SHADOW plots reveal not only the shape of the image at each wavelength but also the dimensions of the image in the horizontal direction and the dispersion of the system. The 30 eV range is spread over approximately 3.57 mm at the carbon edge (Fig. 3 [a - c]), 2.06 mm at the nitrogen edge (Fig. 3. [d - f]), and 1.29 mm at the oxygen edge (Fig. 3 [g - i]). At all wavelengths the horizontal spot size is roughly 2 mm, although the r.m.s. value is much smaller. These dimensions are larger than ideal for the electron imaging system, but they are an inevitable result of using a single grating for a wide energy range.

Although our source model is approximately Gaussian in both space and angle, it does not yet match the accuracy of SHADOW's more complete synchrotron source model. We use a two-dimensional model with few rays to limit computer run-time, while SHADOW uses a complete three-dimensional model with many more rays and a more accurate Gaussian distribution. In order to insure that the resulting image error will not adversely affect the choice of a design, we have slightly modified our choice of source distribution so that our effective r.m.s. widths will be larger than those of SHADOW: when the optimizer differs significantly from SHADOW, the SHADOW raytrace will produce a smaller spot size and higher resolving power. At the carbon edge (291 eV) the error in the r.m.s. spot size is -23.00%, at the nitrogen edge (407 eV) it is 3.68%, and at the oxygen edge (537 eV) it is 1.26%. The error at the carbon edge is significant, but again the optimizer errs conservatively. We plan future adjustment of the limited ray distribution in the model to better match the full raytrace.

8. CONCLUSION

We have reviewed the assumptions and procedures used in the optimization of a hybrid monochromator/spectrograph VLS system for NEXAFS spectroscopy with particular attention to selection of variables of optimization. Previous VLS systems have been of strictly either spectrograph or monochromator geometry, except that of Koch et al²⁴. The system presented contains the mirror-grating separation (r_2) corresponding to an optimal value of the mirror magnification in the conflict between aberrations and the source-size limit given the choice of aperture size and grating dispersion. For this choice of r_2 , an optimal set of groove pattern coefficients $\{a_1, a_2, a_3\}$ has also been found. Even though VLS systems in general offer good focusing over a wide wavelength range, the design problem becomes more difficult and interesting when squeezing an entire NEXAFS snapshot onto a small, (assumed) homogeneous sample, and insisting that one grating focus all three edges by rotating to three "click stop" positions. Despite these challenges, the method presented produces excellent systems. Further, this method is easily applied to other energy ranges--the use of multiple VLS gratings, each optimized for several edges, should allow simultaneous recording of "entire edge" NEXAFS spectra over the full soft x-ray range.

9. ACKNOWLEDGMENTS

The authors wish to thank Christopher Palmer for his critical reading of the manuscript. This work was supported in part by the Director, Office of Energy Research, Office of Basic Energy Sciences, Material Sciences Division of the U.S. Department of Energy under Contract No. DE-AC03-76SF00098.

10. REFERENCES

1. F. M. Gerasimov, E. A. Yaskovlev, B. V. Koshelev, "Mechanically produced concave stigmatic gratings on spherical surfaces," *Opt. Spektrosk.*, 46, 665-668, 1979.
2. T. Harada, S. Moriyama, T. Kita, "Mechanically ruled stigmatic concave gratings," *Japanese Journal of Applied Physics*, 14, 175-179, 1975.
3. M. C. Hettrick, S. Boyer, R. F. Malina, C. Martin, S. Mrowka, "Extreme Ultraviolet Explorer Spectrometer," *Appl. Opt.*, 24, 1737-1756, 1985.
4. M. C. Hettrick, J. H. Underwood, P. J. Batson, M. J. Eckart, "Resolving Power of 35000 (5 mA) in the Extreme Ultraviolet Employing a Grazing Incidence Spectrometer," *Appl. Opt.*, 27, 200-201, 1988.
5. T. Harada, M. Itou, T. Kita, "A Grazing-Incidence Monochromator with a Varied-space Plane Grating for Synchrotron Radiation," *Application, Theory and Fabrication of Periodic Structures*, Proc. SPIE, 503, 114-118, 1984.
6. T. Harada, T. Kita, M. Itou, H. Taira, "Mechanically-Ruled Diffraction Gratings for Synchrotron Radiation," *Nucl. Inst. Meth.*, A246, 272-277, 1986.

7. T. Harada, "Design and Application of a Varied-Space Plane Grating Monochromator for Synchrotron Radiation," Nucl. Instr. Meth., A291, 179-184, 1990.
8. M. Koike, T. Namioka, "High-resolution grazing incidence plane grating monochromator for undulator radiation," Rev. Sci. Instrum., 66, 2144-2146, 1995.
9. M. Koike, R. Beguiristain, J. H. Underwood, T. Namioka, "A new optical design method and its application to an EUV varied line spacing plane grating," Nucl. Instr. and Methods, A347, 273-277, 1994.
10. M. Bissen, M. Fisher, G. Rogers, D. Eisert, K. Kleman, T. Nelson, B. Mason, F. Middleston, H. Hoehst, "First Results of SRC's New High-Energy Resolution Variable Line Density Grating Monochromator Beamline: HERMON," Rev. Sci. Instrum., 66, 2072-2074, 1995.
11. H. Höchst, M. Bissen, M. A. Engelhardt, D. Crossley, "Design study of a high resolution soft x-ray monochromator with a movable variable density grating," Nucl. Instrum. Meth., A319, 121-127, 1992.
12. A. Asfaw, D. L. Ederer, L. Zhou, L. Lin, K. Osborn, T. A. Callcott, M. E. Miyano, E. Morikawa, "Variable Groove Spaced Grating Monochromator for Soft X-ray Emission Spectroscopy at CAMD/LSU," Rev. Sci. Instrum., 66, 1627-1629, 1995.
13. J. Stöhr, *NEXAFS Spectroscopy*, Springer-Verlag, Berlin, 1994.
14. H.C. Gerritsen, H. Van Brug, M. Beerlage, M. J. Van Der Weil, "A polychromator for (S)EXAFS using a laser generated plasma as soft x-ray source," Nucl. Instrum. and Meth., A 238, 546- 553, 1986.
15. B. P. Tonner, G. R. Harp, S. F. Koranda, Z. Zhang, "An electrostatic microscope for synchrotron radiation x-ray absorption microspectroscopy," Rev. Sci. Instrum., 63, 564-568, 1992.
16. P. Kirkpatrick, A. V. Baez, "Formation of Optical Images in X-rays," JOSA, 38, 766-774, 1948.
17. C. Palmer, W. R. McKinney, "Imaging theory of plane-symmetric varied line-spacing grating systems," Opt. Eng., 33, 820-829, 1994.
18. W. McKinney, C. Palmer, "Numerical design method for aberration-reduced concave grating spectrometers," Applied Optics, 26, 3108-3118, 1987.
19. M. S. Caceci, W. P. Cacheris, "Fitting Curves to Data," Byte, 340-362, 1984.
20. C. A. Palmer, "The Theory of Second Generation Holographic Diffraction Gratings," M. A. thesis, Bryn Mawr College, 1988.
21. F. Cerrina, C. Welnak, G. J. Chen, M. Sanchez del Rio, *SHADOW*, Center for X-ray Lithography, Madison, Wisconsin, 1995.
22. W. R. McKinney, "Varied line-space gratings and applications," Rev. Sci. Instr., 63, 1410-1414, 1992.
23. J. H. Underwood, E. M. Gullikson, M. Koike, P. J. Batson, P. E. Denham, K. D. Franck, R. E. Tackaberry, W. F. Steele, "Calibration and standards beamline 6.3.2 at the Advanced Light Source," Rev. Sci. Instrum., in press, 1996.
24. J. A. Koch, B. J. MacGowan, L. B. Da Silva, D. L. Matthews, J. H. Underwood, P. J. Batson, R. W. Lee, R. A. London, S. Mrowka, "Experimental and theoretical investigation of neonlike selenium x-ray laser spectral linewidths and their variation with amplification," Phys. Rev. A, 50, 1877-1898, 1994.

**ERNEST ORLANDO LAWRENCE BERKELEY NATIONAL LABORATORY
ONE CYCLOTRON ROAD | BERKELEY, CALIFORNIA 94720**